

UC Davis

UC Davis Previously Published Works

Title

Engineered Fibrin Gels for Parallel Stimulation of Mesenchymal Stem Cell Proangiogenic and Osteogenic Potential

Permalink

<https://escholarship.org/uc/item/02t0383v>

Journal

Annals of Biomedical Engineering, 43(8)

ISSN

0145-3068

Authors

Murphy, Kaitlin C
Hughbanks, Marissa L
Binder, Bernard YK
[et al.](#)

Publication Date

2015-08-01

DOI

10.1007/s10439-014-1227-x

Peer reviewed



Published in final edited form as:

Ann Biomed Eng. 2015 August ; 43(8): 2010–2021. doi:10.1007/s10439-014-1227-x.

Engineered Fibrin Gels for Parallel Stimulation of Mesenchymal Stem Cell Proangiogenic and Osteogenic Potential

Kaitlin C. Murphy¹, Marissa L. Hughbanks¹, Bernard Y.K. Binder¹, Caroline B. Vissers, and J. Kent Leach^{1,2,*}

¹Department of Biomedical Engineering, University of California, Davis, Davis, CA 95616

²Department of Orthopaedic Surgery, School of Medicine, University of California, Davis Sacramento CA 95817

Abstract

Mesenchymal stem/stromal cells (MSCs) are under examination for use in cell therapies to repair bone defects resulting from trauma or disease. MSCs secrete proangiogenic cues and can be induced to differentiate into bone-forming osteoblasts, yet there is limited evidence that these events can be achieved in parallel. Manipulation of the cell delivery vehicle properties represents a candidate approach for directing MSC function in bone healing. We hypothesized that the biophysical properties of a fibrin gel could simultaneously regulate the proangiogenic and osteogenic potential of entrapped MSCs. Fibrin gels were formed by supplementation with NaCl (1.2, 2.3, and 3.9% w/v) to modulate gel biophysical properties without altering protein concentrations. MSCs entrapped in 1.2% w/v NaCl gels were the most proangiogenic *in vitro*, yet cells in 3.9% w/v gels exhibited the greatest osteogenic response. Compared to the other groups, MSCs entrapped in 2.3% w/v gels provided the best balance between proangiogenic potential, osteogenic potential, and gel contractility. The contribution of MSCs to bone repair was then examined when deployed in 2.3% w/v NaCl gels and implanted into an irradiated orthotopic bone defect. Compared to acellular gels after 3 weeks of implantation, defects treated with MSC-loaded fibrin gels exhibited significant increases in vessel density, early osteogenesis, superior morphology, and increased cellularity of repair tissue. Defects treated with MSC-loaded gels exhibited increased bone formation after 12 weeks compared to blank gels. These results confirm that fibrin gel properties can be modulated to simultaneously promote both the proangiogenic and osteogenic potential of MSCs, and fibrin gels modified by supplementation with NaCl are promising carriers for MSCs to stimulate bone repair *in vivo*.

Keywords

Fibrin; mesenchymal stem cell; angiogenesis; osteogenesis; hydrogel

Address for correspondence: J. Kent Leach, Ph.D., University of California, Davis, Department of Biomedical Engineering, 451 Health Sciences Drive, Genome and Biomedical Sciences Facility, Room 2303, Davis, CA 95616, Phone: (530) 754-9149, Fax: (530) 754-5739, jkleach@ucdavis.edu.

DISCLOSURE STATEMENT

The authors indicate no potential conflicts of interest.

INTRODUCTION

Autologous bone grafting, commonly from the iliac crest, represents the current “gold standard” for bone replacement.¹ However, with most large defects, the supply of autogenous graft is frequently insufficient. Additionally, significant morbidity has been reported with aggressive harvests of autogenous bone, and several studies report frequent complications from iliac crest harvest including donor site pain and injury to cutaneous nerves resulting in painful neuromas.^{2–4} Bioengineering approaches to overcome these problems include the development and application of novel biomaterials, gene therapy, protein delivery, and cell therapies.⁵ Among cells with therapeutic potential, mesenchymal stem/stromal cells (MSCs) are under widespread investigation due to their proangiogenic and osteogenic potential, which allows them to indirectly contribute to bone repair through the secretion of paracrine-acting endogenous growth factors that mediate vessel formation, as well as directly through mineral deposition.^{6–8} We previously demonstrated that MSC induction toward the osteoblastic lineage impairs their proangiogenic potential *in vitro*, as observed by decreased secretion of growth factors such as vascular endothelial growth factor (VEGF) and others.^{9,10} Therefore, new approaches are necessary to leverage the dual potential of MSCs to contribute to bone repair.

MSCs are commonly osteoinduced by exposure to soluble cues, whether *in vitro* or *in vivo*^{9,11}, but other factors including the biophysical properties of the surrounding matrix have a profound effect on cell phenotype. Beyond composition of the matrix, substrate stiffness can direct MSC lineage specification.¹² MSCs grown in softer hydrogels (4 kPa) facilitate paracrine factor production necessary for endothelial cell ingrowth and capillary invasion¹³, while MSCs grown in stiffer substrates (40 kPa) tend toward osteoblastic differentiation.¹⁴ Thus, the optimal conditions for stimulating neovascularization do not necessarily represent the optimal conditions for osteogenic differentiation of MSCs, motivating the need for careful selection of material properties of the chosen delivery vehicle to ensure success of the implanted MSCs. Hydrogels derived from natural polymers such as alginate and collagen have been widely investigated for bone healing.^{15–17} Fibrin is a naturally occurring biomaterial that acts as a scaffold for leukocytes and endothelial cells while tissue formation or regeneration is occurring in the body. Fibrin substrates provide endogenous physical and soluble cues to initiate tissue repair when cells encounter this provisional matrix.¹⁸ Furthermore, biodegradable hydrogels of fibrin can be fabricated into implantable or injectable cell carriers and may be tuned to different compliances.¹⁸ While a variety of methods exist to manipulate the physical properties of fibrin gels, we demonstrated that supplementing the pre-gel solution with varied concentrations of sodium chloride (NaCl) alters a wide array of material properties including gel stiffness, pore size, and fiber diameter.¹⁹ We observed greater compressive moduli, together with decreasing pore size and fiber diameter, as we increased NaCl content up to 3.5% (w/v), above which the biophysical properties began to revert. Our previous studies demonstrated that 1) all salt was eluted from the gel in less than 24 hours; 2) the salt concentrations are not harmful to entrapped cells, and 3) the finalized gel architecture and not magnitude of NaCl concentration was the primary contributor to cell response. While the role of individual ions on fibrin clot physiology is complex and not entirely understood, these changes were

sufficient to modulate the osteogenic response of entrapped MSCs. As MSCs possess dual potential to contribute to bone formation⁶⁻⁸, our goal was to use fibrin gels as the stimulus to direct this dual potential.

We hypothesized that the proangiogenic and osteogenic potential of entrapped MSCs could be simultaneously enhanced by tuning the biophysical properties of fibrin gels through supplementation with NaCl, thus enhancing their indirect and direct contributions toward bone healing in parallel. To explore this hypothesis, we entrapped human MSCs within fibrin gels formed with 1.2–3.9% (w/v) NaCl, formulations previously exhibiting changes in biophysical properties and the capacity to promote osteogenesis *in vitro*¹⁹. We assessed compressive stiffness, contractility, and endogenous proangiogenic growth factor secretion and early and late markers of bone formation *in vitro* in the absence of inductive cues in culture. From these experiments, a single fibrin gel formulation was examined as a carrier vehicle for human MSCs when used to promote bone healing of irradiated calvarial bone defects *in vivo*.

MATERIALS AND METHODS

Cell culture

Human bone marrow-derived MSCs (Lonza, Walkersville, MD) were used without additional characterization. MSCs were expanded in standard culture conditions (37°C, 21% O₂, 5% CO₂) in α -MEM supplemented with 10% fetal bovine serum (FBS, JR Scientific, Woodland, CA) and 1% penicillin/streptomycin (P/S, Mediatech, Herndon, VA) until use at passage 4–5. When entrapped in fibrin gels, MSCs were cultured in media containing 50% α -MEM and 50% growth factor-deficient EGM-2 (EBM-2, Lonza; 10% FBS, 1% P/S, hydrocortisone, gentamycin-1000, EGF, and heparin) as previously reported²⁰ to compare to future co-culture studies with endothelial cells.

Human umbilical cord blood endothelial colony forming cells (ECFCs) were isolated using a protocol approved by the Institutional Review Board of the Indiana University School of Medicine as previously described.²¹ Adherent ECFCs were cultured under standard conditions in T-75 culture flasks coated with 5 μ g/cm² rat tail collagen I (BD Biosciences, San Jose, CA) in complete EGM-2 (10% FBS, 1% P/S, hydrocortisone, gentamycin-1000, EGF, VEGF, FGF, IGF, and heparin).

Fibrin gel preparation

Fibrin gels were formed as we previously described.^{19,22} This fabrication process resulted in fibrin gels with a final fibrinogen concentration of 20 mg/mL (Calbiochem, Gibbstown, NJ), 1.2–3.9% (w/v) NaCl (Sigma Aldrich, St. Louis, MO), 2.5 U/mL thrombin (Calbiochem), 20 mM CaCl₂ (Sigma Aldrich), and 250 KIU/mL aprotinin (Santa Cruz Biotechnology, Santa Cruz, CA), all in PBS. MSCs were added to the fibrinogen pre-gel solution (prior to mixing with thrombin and CaCl₂) to achieve a final concentration of 5×10^2 cells/mL in each gel. A total volume of 80 μ L was added to each cylindrical PDMS mold (5 mm in diameter), and the contents were allowed to gel for 1 hour in standard culture conditions. The PDMS sheet was then carefully lifted from the culture dish, leaving behind the undisturbed fibrin gels,

and the gels were transferred to 12-well tissue culture plates containing media. All gels were cultured in a 1:1 mixture of α -MEM and EBM-2 without osteogenic supplements or growth factors. The day of gel fabrication was denoted as “Day -1”. Gels were maintained in standard cell culture conditions with media changes every 3 days.

Assessment of mechanical and morphologic properties

The compressive moduli of MSC-containing fibrin gels were measured using an Instron 3345 Compressive Testing System (Norwood, MA, USA). Gels were allowed to swell for 1 hour in PBS, blotted, and then loaded between two flat platens and compressed at 1 mm/min. Compressive moduli were calculated from the linear portions of the force-displacement graph for strain ranging from 0% to 5%.¹⁹

The contraction of fibrin gels due to activity of entrapped MSCs was measured by visually following morphologic changes in gel volume. MSC-containing gels were imaged over 14 days in culture using a Nikon Eclipse TE2000U microscope (Melville, NY) and SpotRT digital camera (Diagnostic Instruments, Sterling Heights, MI). The major and minor axes of each construct were measured using ImageJ, and the overall area was calculated.

MSC response to engineered fibrin gels *in vitro*: proangiogenic potential and osteogenic differentiation

MSC secretion of VEGF was quantitatively determined from the conditioned media of MSC-containing fibrin gels at designated time points. Media were refreshed 24 hours before collection, and the concentration of VEGF was determined using a human-specific VEGF ELISA kit (R&D Systems, Minneapolis, MN) according to the manufacturer’s instructions.

To test the bioactivity of MSC conditioned media, the mitogenic response of ECFCs to proangiogenic stimuli was determined as previously described.⁹ Briefly, ECFCs were seeded at 7,500 cells/cm² in EGM-2 in 12-well collagen-coated culture plates and allowed to attach overnight. The next day, culture media was refreshed with a 1:4 volume ratio of MSC-conditioned media (collected at 7 days of culture in fibrin gels) to growth factor-deficient EGM-2 and cultured for 72 hours. Each well was then rinsed with PBS to remove non-adherent cells and debris. Proliferation was analyzed using the Quant-iT PicoGreen dsDNA Assay Kit (Invitrogen, Carlsbad, CA). Cells cultured in complete EGM-2 served as the positive control, while cells cultured in EBM-2 served as the negative control.

We measured the chemotactic response of ECFCs using 24-well FluoroBlok™ inserts (3 μ m pore size, BD Bioscience) coated with a thin layer of gelatin solution (0.1% fish oil gelatin, Sigma Aldrich).^{23,24} ECFCs (300,000 cells/well) were seeded on the top of the transwell inserts in 300 μ L 1:4 unconditioned α -MEM to growth factor-deficient EGM-2. Transwell inserts were then placed over 1 mL 1:4 conditioned α -MEM (collected at 7 days of culture in fibrin gels) to growth factor-deficient EGM-2 to create a positive chemotactic gradient. The no-gradient control consisted of 1 mL growth factor-deficient EGM-2. Plates were then incubated for 24 hours. Cells that migrated through the transwell insert were stained *via* calcein AM (3 mg/mL in PBS) for 30 min, and fluorescence was quantitated using a microplate reader (Synergy HTTR) at 485/530 nm.

The osteogenic response of MSCs entrapped within engineered fibrin gels was assessed from gels collected at 0, 7, and 14 days. Gels were rinsed in PBS and sonicated in 400 μ L passive lysis buffer (Promega, Madison, WI). Samples were centrifuged at 5000 rpm for 10 min to pellet the cell debris, and the supernatant was collected. The supernatant was analyzed for intracellular alkaline phosphatase (ALP) activity using a *p*-nitrophenyl phosphate (PNPP) colorimetric assay, and cell-secreted mineral within fibrin hydrogels was measured using *o*-cresolphthalein complexone as previously described.^{19,25} DNA content was assayed from the supernatant using the Quant-iT PicoGreen dsDNA Assay Kit.

Calvarial defect model

We tested the capacity of MSC-entrapped engineered fibrin gels to stimulate vascularization and bone repair in a bilateral irradiated calvarial bone defect.^{26–28} This model was selected due to the impaired bone healing response and potential to have an internal acellular fibrin gel control for each animal. Treatment of all experimental animals was in accordance with UC Davis animal care guidelines and all National Institutes of Health animal handling protocols. Two weeks prior to the surgical procedure, radiation was delivered to the future surgical site of 11-week-old male nude rats.^{26–28} During the radiation treatment, rats were anesthetized (4%) and maintained (2–3%) by aerosolized isoflurane. A single 12-Gy dose from a Varian 2100C linear accelerator was delivered to D_{\max} at a source-to-skin distance of 80 cm in the Center for Companion Animal Health at the UC Davis School of Veterinary Medicine. The pharynx and the rest of the body were shielded by a combination of beam collimation and a multileaf collimator. Animals were monitored closely for side effects, of which none were apparent.

Fibrin gels containing 2.3% NaCl (w/v) were prepared one day prior to surgery and maintained in media overnight. For surgery, animals were anesthetized (4%) and maintained (2–3%) by aerosolized isoflurane. A mid-longitudinal, 15 mm skin incision was made on the dorsal surface of the cranium, and care was taken to ensure that the periosteum was completely cleared from the surface of the cranial bone by scraping. A trephine bur was used to create one circular 3.5 mm diameter defect in the rat cranium on both sides of the sagittal suture. The full thickness (~1–1.5 mm) of the cranial bone was removed and replaced immediately with a fibrin gel. Every animal received an acellular fibrin gel as a control.

Non-invasive analysis of tissue neovascularization

Blood flow was measured on anesthetized animals immediately postoperatively and 5, 14, and 21 days after surgery using a Periscan PIM 3 laser Doppler blood perfusion imager (Perimed, Stockholm, Sweden).²⁶ To ensure accurate measurements, the hair covering the surgical site was removed the day before scanning with a depilatory, after which all traces of the depilatory were removed with alcohol wipes. Perfusion measurements were obtained from a 7.5 \times 13 mm rectangle superimposed over the defect and surrounding half of the cranium. To minimize variability, perfusion index was normalized to the post-operative values for each animal.

Histological staining and analysis of neovascularization

Animals were euthanized after 3 weeks by CO₂ inhalation and their calvariae removed (n=6 per group). Recovered bone tissues were fixed in phosphate-buffered formalin for 48 hours, after which they were demineralized in Calci-Clear (National Diagnostics, Atlanta, GA) for 48 hours and then moved to 70% ethanol for storage before processing and analysis. The calvariae were histologically processed, paraffin embedded, and sectioned at 5 µm thickness.

Sections were stained with hematoxylin and eosin (H&E) and imaged using a Nikon Eclipse TE2000U microscope and SpotRT digital camera. Blood vessels in the entire defect, approximately 20 high-power fields, were counted manually at 100× magnification and normalized to tissue area. Blood vessels were identified as circular structures and well-defined long tubule structures, containing red blood cells, and the number of vessels was normalized to tissue area to determine vascular density. The presence of blood vessels was confirmed by immunohistochemistry (IHC) for rat CD31 (1:100, JC/70A, Pierce Antibody Products, Waltham, MA). The investigator was blinded to the implant type while counting blood vessels. Masson's trichrome stain was performed as previously described to identify collagen within the defect.⁸ In order to visualize cells undergoing osteogenic differentiation, IHC was performed on sections using a primary antibody against osteocalcin (1:200, ab13420, Abcam, Cambridge, MA)²⁹ and a mouse specific HRP/DAB detection kit (ab64259, Abcam).

Analysis of in vivo bone formation

Bone formation was quantified from animals euthanized after 12 weeks (n=6 per group). Calvariae were removed, fixed in phosphate-buffered formalin, and moved to 70% ethanol. Calvarial explants were scanned using a µCT 35 MicroCT scanner (Scanco Medical AG, Bruttisellen, Switzerland) at an energy level of 70 keV, an intensity of 114 µA, 300 msec integration time, three averages, with a 0.5 mm aluminum filter and an isotropic resolution of 15 µm in all three spatial dimensions. Scanning for the calvarium was initiated proximately 1 mm rostral to the defects and extended 1 mm beyond the defect caudally. The right and left defects were evaluated separately. The gray-scale images were segmented using a constrained three-dimensional Gaussian filter (sigma=0.8, support=1.0) and fixed threshold of 191 mg HA/cc to separate mineralized tissue from un-mineralized tissue. Grey scale (x-ray attenuation) was calibrated to density (hydroxyapatite concentration) by calibration of a phantom consisting of 0.0, 99.6, 200.0, 401.0 and 800.3 mg HA/cc concentrations. A cylindrical ROI with the same diameter as the original defect (3.5 mm) and 1.5 mm long was centered in the defect. Total volume (TV) was the volume of the ROI. Bone volume (BV) was defined as the volume of mineralized tissue within the ROI. Bone volume fraction (BVf; BV/TV) and bone mineral density (BMD; mean density of only mineralized material within volume) were used to compare samples.

Statistical analysis

Data are presented as mean ± standard deviation. Statistical analysis was performed using two-way ANOVA with Bonferonni correction for multiple comparisons or paired t-tests when appropriate. All statistical analysis was performed in Prism 6 software (GraphPad); *p* values less than 0.05 were considered statistically significant.

RESULTS

Stiffness and vulnerability to gel contraction is controlled by sodium chloride

MSC-loaded gels prepared with 2.3% NaCl exhibited a significantly greater compressive modulus compared to those prepared with 1.2% or 3.9% NaCl (Fig. 1A), following a similar trend to our previous data analyzing acellular gels.¹⁹ No significant difference in compressive modulus was observed between 1.2% and 3.9% NaCl-containing fibrin gels. Changes in construct morphology were assessed by examining the area of cellular gels over time. After 5 days, all constructs had decreased in diameter, but gels formed with 1.2% NaCl revealed significantly more contraction compared to those formed with 2.3 and 3.9% NaCl. Contraction appeared to plateau in gels formed with 1.2% NaCl after 7 days in culture, while gels formed with 2.3% and 3.9% NaCl continued to contract until 14 days (Fig. 1B, 1C). Interestingly, gels formed with 2.3% NaCl appeared to contract in a more linear, predictable manner over the 14 day examination period, while gels formed with 3.9% NaCl exhibited a lag time of 7 days before significant changes in gel volume were observed.

Response of entrapped MSCs within fibrin gels is dependent upon NaCl content

We quantified the proangiogenic potential of entrapped MSCs within fibrin gels by measuring the endogenous secretion of VEGF₁₆₅, a potent angiogenic growth factor, in the conditioned media. We detected significantly more VEGF produced by MSCs entrapped in fibrin gels formed with 1.2% NaCl at all time points compared to cells entrapped within gels formed with 3.9% NaCl (Fig. 2A). Since biophysical properties of fibrin gels (*e.g.*, fiber diameter, pore size) are modified by NaCl content, VEGF could potentially be retained as a function of salt supplementation. We detected less than 10% of the total VEGF was retained in any formulation (*data not shown*) when measuring residual VEGF in fibrin gels after 7 days of culture. VEGF production increased over time with all fibrin gels, regardless of NaCl content, likely due to MSC proliferation (Fig. 3C). We characterized the functional bioactivity of the secreted growth factors in conditioned media by observing its ability to stimulate proliferation and migration of ECFCs. ECFCs exhibited the greatest proliferation (Fig. 2B) and migration response (Fig. 2C) when stimulated with conditioned medium from fibrin gels formed with 1.2% NaCl, corresponding to the greatest VEGF concentrations. ECFCs exhibited an intermediate response to 2.3% gels, and conditioned media from MSCs in 3.9% gels consistently yielded the weakest ECFC response.

We also measured the osteogenic response of entrapped MSCs to fibrin gels with increasing NaCl content in the absence of soluble osteogenic cues. We detected a direct correlation between ALP activity, an early marker of osteogenic differentiation within osteoblastic cells, and increasing NaCl concentration. After 7 days, MSCs entrapped in fibrin gels formed with 3.9% NaCl had significantly greater ALP activity compared to cells in gels formed with 1.2% NaCl (Fig. 3A). MSCs suspended in gels formed with 1.2% NaCl, which also had the smallest compressive modulus and were most vulnerable to contraction by entrapped cells, had the lowest ALP activity. Regardless of NaCl content, ALP activity peaked in all gels at 7 days and then decreased, indicative of the cyclic nature of ALP in the osteogenic program. Cell secreted mineral, a late stage marker of differentiation and function, exhibited a similar trend to ALP activity. Specifically, fibrin gels formed with 2.3% and 3.9% NaCl contained

more calcium than gels formed with 1.2% NaCl at both 7 and 14 days, with 3.9% NaCl-containing gels stimulating the highest calcium content (Fig. 3B). We observed an inverse correlation between NaCl content and DNA values. Gels formed with higher NaCl concentrations yielded lower DNA concentrations after 7 days, and these differences were more pronounced after 14 days in culture (Fig. 3C). Thus, fibrin gels formed with 2.3% NaCl were used for all subsequent *in vivo* studies in light of *in vitro* data balancing gel contraction, VEGF secretion, and osteogenic differentiation.

Analysis of *in vivo* neovascularization and early bone formation

Immediately after surgery, we analyzed perfusion within the implant site noninvasively using LDPI to provide a reference for subsequent scans. At day 14, we detected significantly increased perfusion by LDPI in defects treated with MSC-containing fibrin gels compared to acellular, blank gels (Fig. 4A, 4B). Perfusion was statistically similar at the other time points. Vessel density within the implant was quantified after 3 weeks by enumerating blood vessels in repair tissue from H&E-stained histological sections and confirmed by immunostaining for CD31 (Fig. 5A,B), where erythrocytes are clearly visible in the lumens. Gels containing MSCs exhibited significantly greater vessel density than blank gels (Fig. 5C). Furthermore, fibrin gels containing MSCs contained more collagen and were appreciably thicker (Fig. 6B,D) than acellular blank gels (Fig. 6A,C). Osteocalcin staining of the explants revealed greater osteoblastic activity in the MSC-containing gels after three weeks (Fig. 6F) compared to the blank gels (Fig. 6E).

Analysis of bone formation *in vivo*

Defects treated with MSC-containing fibrin gels exhibited significant increases in BVF over blank gels after twelve weeks (Fig. 7A,C), following a similar trend observed for neovascularization. However, we did not detect statistical differences in BMD when comparing the treatment groups (Fig. 7B).

DISCUSSION

Successful interventions in bone healing should ideally promote both vascularization to provide nutrients to neighboring cells and mineral deposition to restore strength and integrity to the defect site. MSCs are a promising source for cell therapies in bone repair due to their secretion of proangiogenic cues that recruit vessel-forming endothelial cells and their ability to differentiate into bone-forming osteoblasts. The regulation of the cellular machinery of MSCs through substrate-mediated signaling provides an opportunity to enhance their osteogenic capacity.^{12,30} However, the proangiogenic potential of MSCs decreases as MSCs exhibit a stronger osteoblastic phenotype⁹, thereby compromising the dual potential of MSCs in bone repair. In this study, our objective was to engineer a fibrin gel that could simultaneously support the proangiogenic and osteogenic potential of entrapped MSCs. Our data reveal that supplementation of the fibrin gel with NaCl modulates fibrin gel properties such that a greater balance between these two phenotypes can be achieved.

Fibrin is an attractive biomaterial for cell delivery, as it naturally occurs as a provisional matrix during tissue repair.^{31,32} Other biomacromolecules such as collagen exist in mature tissues and do not actively direct cells to secrete reparative growth factors and extracellular matrix components³³, potentially limiting their efficacy as a cell delivery vehicle for tissue regeneration. The biophysical properties of fibrin gels can be tuned using a variety of techniques including altering protein concentrations, pH, calcium content, and overall ionic strength.³⁴ We have previously shown that changing the NaCl content in the pre-gel solution alters gel stiffness, pore size, fiber diameter, and permeability.¹⁹ Using NaCl to alter the gel properties has two main advantages compared to the more commonly used strategy of increasing protein concentrations: 1) the slow gelation time avoids mechanical stress and osmotic shock on the entrapped cells; and 2) the stiffness may be controlled without drastically deviating from the physiologic concentrations of fibrin and thrombin, thereby enabling the potential for autologous use.³⁵ In this study the stiffness of the fibrin gels composed of 20 mg/mL fibrinogen ranged from 10–20 kPa, adequate moduli for materials applied to non-weight bearing bone in the head and neck region. The increase in substrate stiffness compared to fibrin gels formed in water (5 kPa) is sufficient to drive osteogenesis.^{19,36} Gel stiffness impedes capillary formation within the gel and invasion of host endothelial cells³⁷, a critical factor to consider since bone formation is intertwined with vascularization. Fibril density and matrix stiffness strongly influences the ability of endothelial cells to remodel their surroundings and correlates with the diameter and density of microvessels *in vivo*.³⁸ Thus, it is preferred to keep bulk gel stiffness low in order to enable the dually desired functions of MSCs in bone healing: stimulating neovascularization and differentiation toward the osteoblastic phenotype.

The results of this study confirm that modulation of fibrin gel biophysical properties, achieved through NaCl supplementation and in the absence of osteoinductive soluble cues, can instruct the proangiogenic and osteogenic potential of entrapped MSCs *in vitro*. As NaCl concentration increased, so did the early and late markers of osteogenesis. We also observed decreased cell proliferation and proangiogenic potential as NaCl concentration increased. These data are in agreement with our previous findings⁹ and those of others³⁷ that MSCs of greater osteogenic commitment, achieved through soluble osteogenic supplements, exhibit reduced proangiogenic potential. Our observation of continued increased osteogenic differentiation with increasing salt content differs slightly from our previous study which revealed decreases in ALP activity at the highest NaCl concentrations¹⁹, perhaps due to the presence of osteogenic supplements in the culture medium, while MSCs in this study only received substrate-mediated cues. Others have observed enhanced osteogenic potential of MSCs in fibrin gels through increasing protein concentration³⁹, applying tensile force⁴⁰ and inclusion of osteoconductive materials³⁶. However, these approaches do not strive to balance the osteogenic potential with the proangiogenic potential of the entrapped MSCs.

In addition to directing cell phenotype, we observed that gel contraction drastically increased as NaCl concentration decreased. These data are in agreement with our prior work, which found that the gels formed with the lower NaCl concentrations were most susceptible to cellular contractile forces due to a lower compressive modulus and a higher rate of cell proliferation.¹⁹ The supplementation of fibrinogen with increasing NaCl content yields

fibrin gels with distinct morphological characteristics despite similar initial moduli. These differences could contribute to the vulnerability of gel contraction by entrapped cells. We also reported that another cell type, dorsal root ganglion neurons, upregulated their expression of genes encoding for enzymes that could remodel fibrin gels.⁴¹ Clinically, implants must exhibit minimal contraction in order to integrate with the surrounding tissue during bone healing, as bone ingrowth occurs primarily from the edges of the defect. If implants pull away from the defect margins, the native tissue repair response is impeded because there is insufficient extracellular matrix to provide a scaffolding for host cells to populate. In light of superior proangiogenic response, increased osteogenic potential, and reduced contraction with MSCs in 2.3% NaCl-containing gels, characterized *in vitro* when there are fewer variables contributing to cellular response, we selected the mid-range NaCl concentration to fabricate fibrin hydrogels as a platform for *in vivo* studies. We then sought to determine, for the first time, whether MSCs implanted in NaCl-supplemented fibrin gels could stimulate bone repair in this harsh, nonhealing bone defect.

Radiotherapy is commonly used as primary treatment and as an adjuvant to the surgical excision of in the head and neck region. The resulting tissue microenvironment leads to fibrosis that makes secondary reconstruction of the surgical site difficult. Furthermore, the treatment of extensive osteoradionecrosis, as a side effect of radiotherapy, often requires the removal of large amounts of bone in a previously irradiated field.⁴² While effective in eradicating the damaged cells, previous reports confirm that irradiated defects have severely compromised bone healing due to the impairment in number and activity of endothelial and other tissue-forming cells.^{43,44} Nussenbaum *et al.* reported that in animals receiving radiation 2 weeks prior to surgery, inlay calvarial bone graft failed to heal at the wound margins by 4 weeks after surgery.²⁷ With a clinical eye toward healing irradiated bone defects resulting from head and neck cancer, we selected an irradiated bilateral calvarial defect for our animal model. Our results demonstrate that NaCl-supplemented fibrin gels are effective delivery vehicles for MSCs *in vivo*. Defects treated with MSC-loaded fibrin gels contained repair tissue that was substantially thicker and more robust, containing greater amounts of collagen, than the thin fibrous layers remaining in the defects treated with acellular blank gels. Compared to empty fibrin gels, we observed increased early perfusion for defects treated with MSC-loaded gels using noninvasive imaging, and these findings were supported by enumeration of blood vessels in histological samples of explanted tissues at 3 weeks. Additionally, others have observed that MSCs enhance perfusion, and that this is most likely a result of implanted MSCs secreting trophic factors to recruit surrounding endothelial cells.^{45,46} Although vessel perfusion measured *via* LDPI at 21 days was the same for both MSC-loaded and blank fibrin gels, the vessel count as measured *via* histology at 21 days was significantly greater in MSC-loaded gels compared to the blank fibrin gels. This phenomenon has been observed when delivering recombinant human VEGF *in vivo*, where high doses of VEGF caused rapid initial vessel growth and perfusion, yet eventually resulted in dramatic regression of the neovascularization within three weeks, suggesting that the remaining vessels may not be functional at this time.⁴⁷

After 12 weeks, we observed increased bone formation in defects treated with MSC-containing gels; data that correlate with increases in vascular density at earlier time points

and agree with earlier studies.^{26,28,48} MSC-loaded gels resulted in a two-fold increase in BVF compared to the blank fibrin gels. However, the BMD was not statistically different between the two groups, indicating that the quality of the deposited bone was the same for MSC-containing and blank fibrin gels. However, both groups exhibited a BMD of approximately 800 mg HA/cc, which is only 20% less than native cortical bone⁴⁹ and is similar to what others have observed with MSC treatment.⁵⁰ Together, this implies that while there was limited bony ingrowth, the bone that was deposited was of high quality. As radiation causes tissue regeneration to be severely stunted, later time points should be investigated in the future.

CONCLUSION

The results of this study confirm that NaCl can be used to tailor fibrin gels to support both the proangiogenic and osteogenic potential of MSCs *in vitro*. Furthermore, these biomaterials are effective delivery vehicles for MSCs into orthotopic defects, providing a platform to deliver cells to the defect site, jumpstart healing by stimulating much-needed vascularization, and serving as a vehicle to instruct MSCs *in situ*. This approach is a promising technology to reduce or eliminate the need for costly and inefficient delivery of recombinant growth factors for angiogenesis.

ACKNOWLEDGEMENTS

This work was supported by NIH Grants R03-DE021704 and R21-AG036963 and the AO Foundation (C10-39L) to JKL. This project was also supported by the California Institute for Regenerative Medicine UC Davis Stem Cell Training Program (CIRM T1-00006, CIRM TG2-01163) to BYB. We appreciate the assistance of Michael Kent, DVM, PhD, for his help in irradiating the animals and Mervin Yoder, M.D., for providing endothelial colony forming cells.

REFERENCES

1. Khan SN, Cammisa FP Jr, Sandhu HS, Diwan AD, Girardi FP, Lane JM. The biology of bone grafting. *J Am Acad Orthop Surg.* 2005; 13(1):77–86. [PubMed: 15712985]
2. Seiler JG 3rd, Johnson J. Iliac crest autogenous bone grafting: donor site complications. *J South Orthop Assoc.* 2000; 9(2):91–97. [PubMed: 10901646]
3. Arrington ED, Smith WJ, Chambers HG, Bucknell AL, Davino NA. Complications of iliac crest bone graft harvesting. *Clin Orthop Relat Res.* 1996; (329):300–309. [PubMed: 8769465]
4. Silber JS, Anderson DG, Daffner SD, Brislin BT, Leland JM, Hilibrand AS, Vaccaro AR, Albert TJ. Donor site morbidity after anterior iliac crest bone harvest for single-level anterior cervical discectomy and fusion. *Spine.* 2003; 28(2):134–139. [PubMed: 12544929]
5. Stegemann JP, Verrier S, Gebhard F, Laschke MW, Martin I, Simpson H, Miclau T. Cell therapy for bone repair: narrowing the gap between vision and practice. *Eur Cell Mater.* 2014; 27:1–4. [PubMed: 24802610]
6. Bruder SP, Kurth AA, Shea M, Hayes WC, Jaiswal N, Kadiyala S. Bone regeneration by implantation of purified, culture-expanded human mesenchymal stem cells. *J Orthop Res.* 1998; 16(2):155–162. [PubMed: 9621889]
7. Kanczler JM, Oreffo RO. Osteogenesis and angiogenesis: the potential for engineering bone. *Eur Cell Mater.* 2008; 15:100–114. [PubMed: 18454418]
8. Bhat A, Hoch AI, Decaris ML, Leach JK. Alginate hydrogels containing cell-interactive beads for bone formation. *FASEB J.* 2013; 27(12):4844–4852. [PubMed: 24005905]
9. Hoch AI, Binder BY, Genetos DC, Leach JK. Differentiation-dependent secretion of proangiogenic factors by mesenchymal stem cells. *PLoS One.* 2012; 7(4):e35579. [PubMed: 22536411]

10. Binder BY, Genetos DC, Leach JK. Lysophosphatidic acid protects human mesenchymal stromal cells from differentiation-dependent vulnerability to apoptosis. *Tissue Eng Part A*. 2014; 20(7–8): 1156–1164. [PubMed: 24131310]
11. Dosier CR, Uhrig BA, Willett NJ, Krishnan L, Li MT, Stevens HY, Schwartz Z, Boyan BD, Guldborg RE. Effect of cell origin and timing of delivery for stem cell-based bone tissue engineering using biologically functionalized hydrogels. *Tissue Eng Part A*. 2014
12. Engler AJ, Sen S, Sweeney HL, Discher DE. Matrix elasticity directs stem cell lineage specification. *Cell*. 2006; 126(4):677–689. [PubMed: 16923388]
13. Ghajar CM, Blevins KS, Hughes CC, George SC, Putnam AJ. Mesenchymal stem cells enhance angiogenesis in mechanically viable prevascularized tissues via early matrix metalloproteinase upregulation. *Tissue Eng*. 2006; 12(10):2875–2888. [PubMed: 17518656]
14. Xue R, Li JY, Yeh Y, Yang L, Chien S. Effects of matrix elasticity and cell density on human mesenchymal stem cells differentiation. *J Orthop Res*. 2013; 31(9):1360–1365. [PubMed: 23606500]
15. Lee KY, Mooney DJ. Hydrogels for tissue engineering. *Chem Rev*. 2001; 101(7):1869–1879. [PubMed: 11710233]
16. Annabi N, Tamayol A, Uquillas JA, Akbari M, Bertassoni LE, Cha C, Camci-Unal G, Dokmeci MR, Peppas NA, Khademhosseini A. 25th anniversary article: Rational design and applications of hydrogels in regenerative medicine. *Adv Mater*. 2014; 26(1):85–123. [PubMed: 24741694]
17. Salinas CN, Anseth KS. Mesenchymal stem cells for craniofacial tissue regeneration: designing hydrogel delivery vehicles. *J Dent Res*. 2009; 88(8):681–692. [PubMed: 19734453]
18. Ahmed TA, Dare EV, Hincke M. Fibrin: a versatile scaffold for tissue engineering applications. *Tissue Eng Part B Rev*. 2008; 14(2):199–215. [PubMed: 18544016]
19. Davis HE, Miller SL, Case EM, Leach JK. Supplementation of fibrin gels with sodium chloride enhances physical properties and ensuing osteogenic response. *Acta Biomater*. 2011; 7(2):691–699. [PubMed: 20837168]
20. Kang KT, Allen P, Bischoff J. Bioengineered human vascular networks transplanted into secondary mice reconnect with the host vasculature and re-establish perfusion. *Blood*. 2011; 118(25):6718–6721. [PubMed: 22039257]
21. Yoder MC, Mead LE, Prater D, Krier TR, Mroueh KN, Li F, Krasich R, Temm CJ, Prchal JT, Ingram DA. Redefining endothelial progenitor cells via clonal analysis and hematopoietic stem/progenitor cell principals. *Blood*. 2007; 109(5):1801–1809. [PubMed: 17053059]
22. Murphy KC, Leach JK. A reproducible, high throughput method for fabricating fibrin gels. *BMC Res Notes*. 2012; 5:423. [PubMed: 22873708]
23. Decaris ML, Lee CI, Yoder MC, Tarantal AF, Leach JK. Influence of the oxygen microenvironment on the proangiogenic potential of human endothelial colony forming cells. *Angiogenesis*. 2009; 12(4):303–311. [PubMed: 19544080]
24. Jose S, Hughbanks ML, Binder BY, Ingavle GC, Leach JK. Enhanced trophic factor secretion by mesenchymal stem/stromal cells with Glycine-Histidine-Lysine (GHK)-modified alginate hydrogels. *Acta Biomater*. 2014; 10(5):1955–1964. [PubMed: 24468583]
25. Decaris ML, Leach JK. Design of experiments approach to engineer cell-secreted matrices for directing osteogenic differentiation. *Ann Biomed Eng*. 2011; 39(4):1174–1185. [PubMed: 21120695]
26. Kaigler D, Wang Z, Horger K, Mooney DJ, Krebsbach PH. VEGF scaffolds enhance angiogenesis and bone regeneration in irradiated osseous defects. *J Bone Miner Res*. 2006; 21(5):735–744. [PubMed: 16734388]
27. Nussenbaum B, Rutherford RB, Krebsbach PH. Bone regeneration in cranial defects previously treated with radiation. *Laryngoscope*. 2005; 115(7):1170–1177. [PubMed: 15995502]
28. Leu A, Stieger SM, Dayton P, Ferrara KW, Leach JK. Angiogenic response to bioactive glass promotes bone healing in an irradiated calvarial defect. *Tissue Eng Part A*. 2009; 15(4):877–885. [PubMed: 18795867]
29. Shih YR, Hwang Y, Phadke A, Kang H, Hwang NS, Caro EJ, Nguyen S, Siu M, Theodorakis EA, Gianneschi NC, et al. Calcium phosphate-bearing matrices induce osteogenic differentiation of

- stem cells through adenosine signaling. *Proc Natl Acad Sci U S A*. 2014; 111(3):990–995. [PubMed: 24395775]
30. McBeath R, Pirone DM, Nelson CM, Bhadriraju K, Chen CS. Cell shape, cytoskeletal tension, and RhoA regulate stem cell lineage commitment. *Dev Cell*. 2004; 6(4):483–495. [PubMed: 15068789]
 31. Janmey PA, Winer JP, Weisel JW. Fibrin gels and their clinical and bioengineering applications. *J R Soc Interface*. 2009; 6(30):1–10. [PubMed: 18801715]
 32. Barsotti MC, Magera A, Armani C, Chiellini F, Felice F, Dinucci D, Piras AM, Minnocci A, Solaro R, Soldani G, et al. Fibrin acts as biomimetic niche inducing both differentiation and stem cell marker expression of early human endothelial progenitor cells. *Cell Prolif*. 2011; 44(1):33–48. [PubMed: 21199008]
 33. Grassl ED, Oegema TR, Tranquillo RT. Fibrin as an alternative biopolymer to type-I collagen for the fabrication of a media equivalent. *J Biomed Mater Res*. 2002; 60(4):607–612. [PubMed: 11948519]
 34. Blomback B, Bark N. Fibrinopeptides and fibrin gel structure. *Biophys Chem*. 2004; 112(2–3): 147–151. [PubMed: 15572242]
 35. Alston SM, Solen KA, Broderick AH, Sukavaneshvar S, Mohammad SF. New method to prepare autologous fibrin glue on demand. *Transl Res*. 2007; 149(4):187–195. [PubMed: 17383592]
 36. Davis HE, Binder BY, Schaecher P, Yakoobinsky DD, Bhat A, Leach JK. Enhancing osteoconductivity of fibrin gels with apatite-coated polymer microspheres. *Tissue Eng Part A*. 2013; 19(15–16):1773–1782. [PubMed: 23560390]
 37. Kniazeva E, Kachgal S, Putnam AJ. Effects of extracellular matrix density and mesenchymal stem cells on neovascularization in vivo. *Tissue Eng Part A*. 2011; 17(7–8):905–914. [PubMed: 20979533]
 38. Critser PJ, Kreger ST, Voytik-Harbin SL, Yoder MC. Collagen matrix physical properties modulate endothelial colony forming cell-derived vessels in vivo. *Microvasc Res*. 2010; 80(1):23–30. [PubMed: 20219180]
 39. Catelas I, Sese N, Wu BM, Dunn JC, Helgerson S, Tawil B. Human mesenchymal stem cell proliferation and osteogenic differentiation in fibrin gels in vitro. *Tissue Eng*. 2006; 12(8):2385–2396. [PubMed: 16968177]
 40. Sasaki JI, Matsumoto T, Imazato S. Oriented bone formation using biomimetic fibrin hydrogels with three-dimensional patterned bone matrices. *J Biomed Mater Res A*. 2014
 41. Man AJ, Davis HE, Itoh A, Leach JK, Bannerman P. Neurite outgrowth in fibrin gels is regulated by substrate stiffness. *Tissue Eng Part A*. 2011; 17(23–24):2931–2942. [PubMed: 21882895]
 42. Hu WW, Ward BB, Wang Z, Krebsbach PH. Bone regeneration in defects compromised by radiotherapy. *J Dent Res*. 2010; 89(1):77–81. [PubMed: 19966040]
 43. Dorresteijn LD, Kappelle AC, Boogerd W, Klokman WJ, Balm AJ, Keus RB, van Leeuwen FE, Bartelink H. Increased risk of ischemic stroke after radiotherapy on the neck in patients younger than 60 years. *J Clin Oncol*. 2002; 20(1):282–288. [PubMed: 11773180]
 44. Jacobsson M, Albrektsson T, Turesson I. Dynamics of irradiation injury to bone tissue. A vital microscopic investigation. *Acta Radiol Oncol*. 1985; 24(4):343–350. [PubMed: 2994392]
 45. Kagiwada H, Yashiki T, Ohshima A, Tadokoro M, Nagaya N, Ohgushi H. Human mesenchymal stem cells as a stable source of VEGF-producing cells. *J Tissue Eng Regen Med*. 2008; 2(4):184–189. [PubMed: 18452238]
 46. He J, Genetos DC, Leach JK. Osteogenesis and trophic factor secretion are influenced by the composition of hydroxyapatite/poly(lactide-co-glycolide) composite scaffolds. *Tissue Eng Part A*. 2010; 16(1):127–137. [PubMed: 19642853]
 47. Davies N, Dobner S, Bezuidenhout D, Schmidt C, Beck M, Zisch AH, Zilla P. The dosage dependence of VEGF stimulation on scaffold neovascularisation. *Biomaterials*. 2008; 29(26): 3531–3538. [PubMed: 18541296]
 48. Nguyen LH, Annabi N, Nikkhah M, Bae H, Binan L, Park S, Kang Y, Yang Y, Khademhosseini A. Vascularized bone tissue engineering: approaches for potential improvement. *Tissue Eng Part B Rev*. 2012; 18(5):363–382. [PubMed: 22765012]

49. Umoh JU, Sampaio AV, Welch I, Pitelka V, Goldberg HA, Underhill TM, Holdsworth DW. In vivo micro-CT analysis of bone remodeling in a rat calvarial defect model. *Phys Med Biol.* 2009; 54(7):2147–2161. [PubMed: 19287088]
50. Deshpande SS, Gallagher KK, Donneys A, Tchanque-Fossuo CN, Sarhaddi D, Sun H, Krebsbach PH, Buchman SR. Stem cell therapy remediates reconstruction of the craniofacial skeleton after radiation therapy. *Stem Cells Dev.* 2013; 22(11):1625–1632. [PubMed: 23282102]

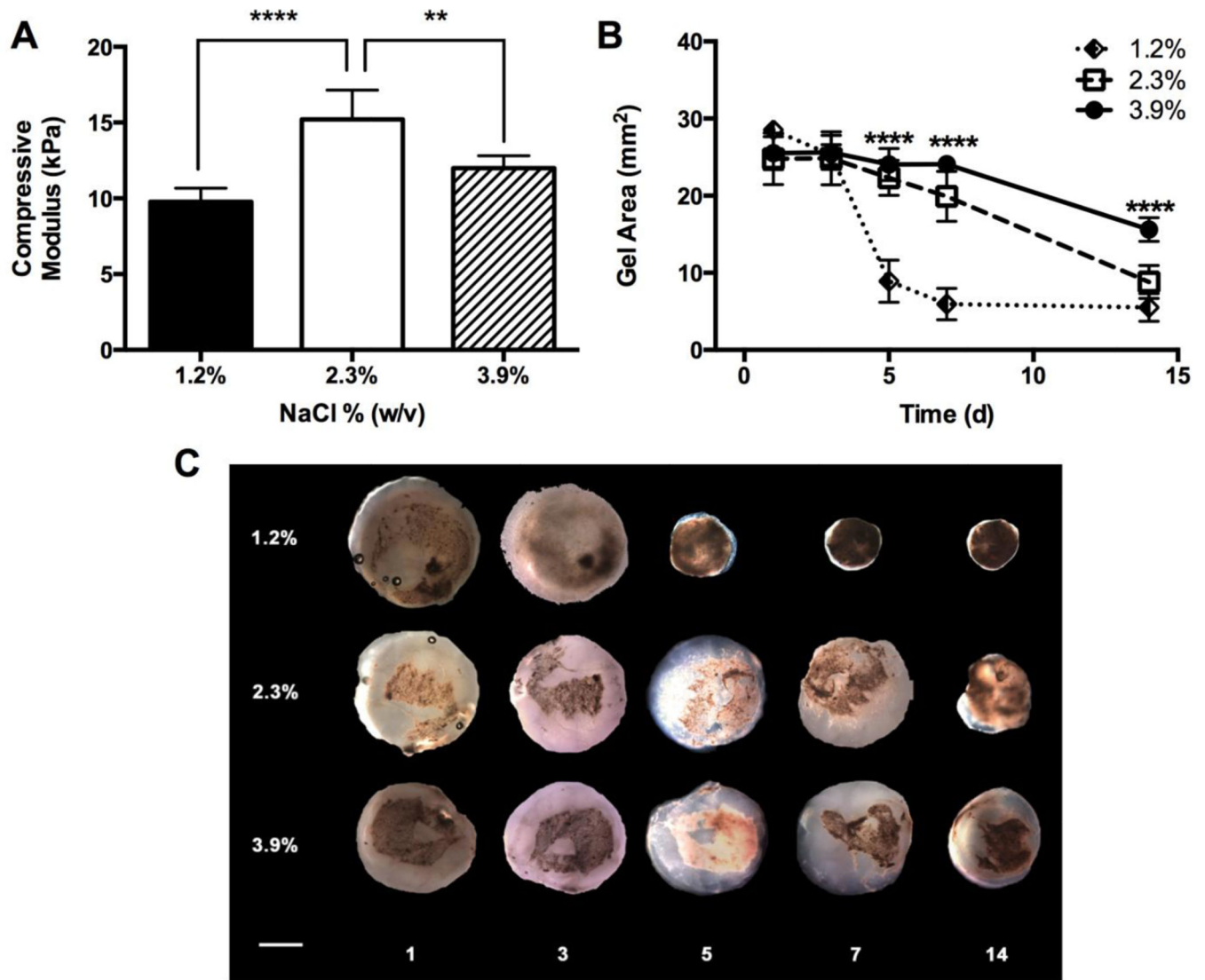


Figure 1. Biomechanical properties and hydrogel morphology of MSC-loaded fibrin gels are dependent upon salt concentration. (A) Compressive modulus of gels ($n=4$; **** $p<0.0001$ vs. 1.2%, ** $p<0.01$ vs. 3.9%); (B) quantification of gel contraction over time ($n=3$; **** $p<0.0001$ vs. 3.9%); and (C) representative images of fibrin gels over time. Scale bar represents 2 mm.

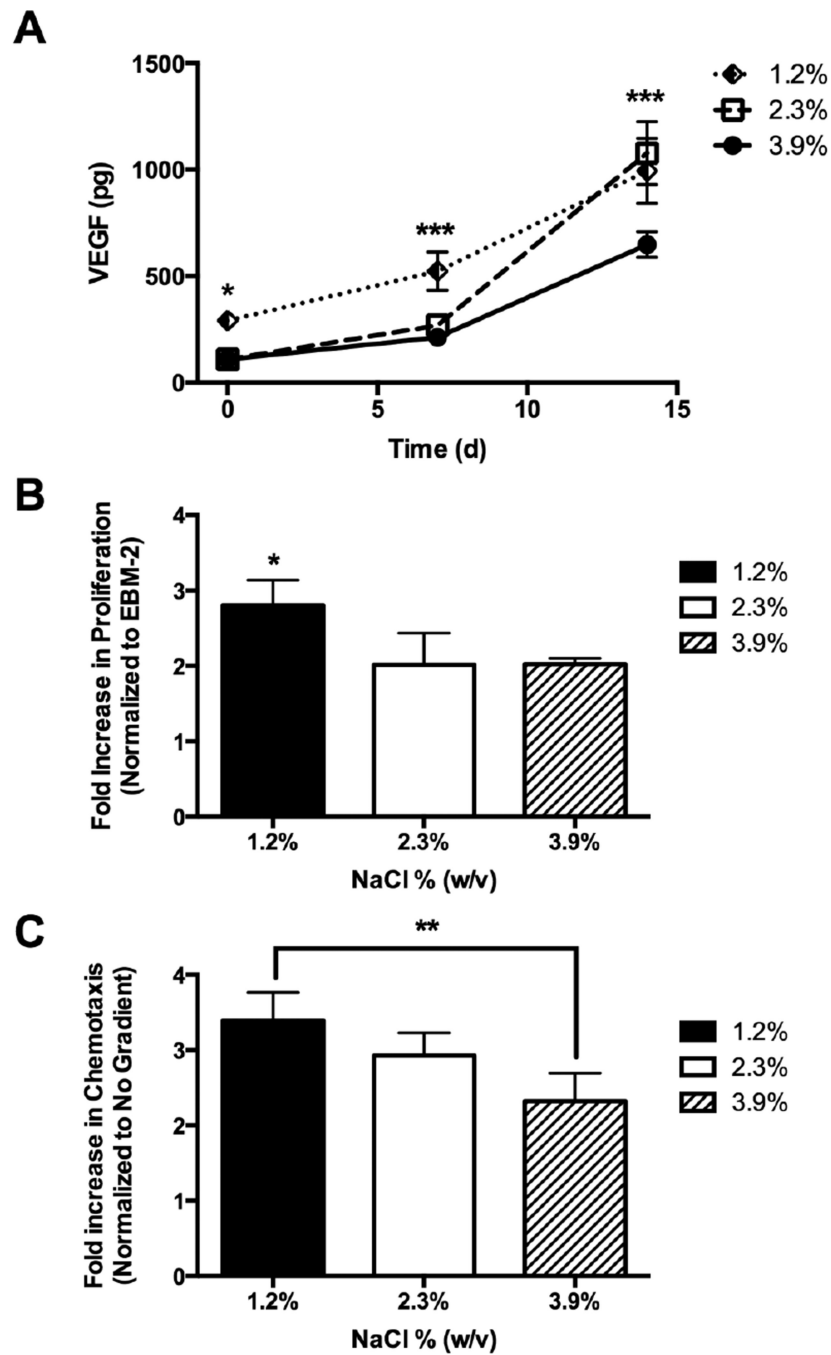


Figure 2. Secretion of endogenous proangiogenic growth factors is inversely related to salt content. (A) VEGF concentration in conditioned media ($n=3$, $*p<0.05$ vs. 2.3% and 3.9%, $***p<0.001$ vs. 2.3% and 3.9%) at designated time points in culture; (B) fold increase in proliferation normalized to EBM-2 using conditioned medium collected at 7 days ($n=4$, $*p<0.05$ vs. 2.3% and 3.9%); and (C) fold increase in chemotaxis normalized to no gradient using conditioned medium collected at 7 days ($n=4$, $**p<0.01$ vs. 2.3% and 3.9%).

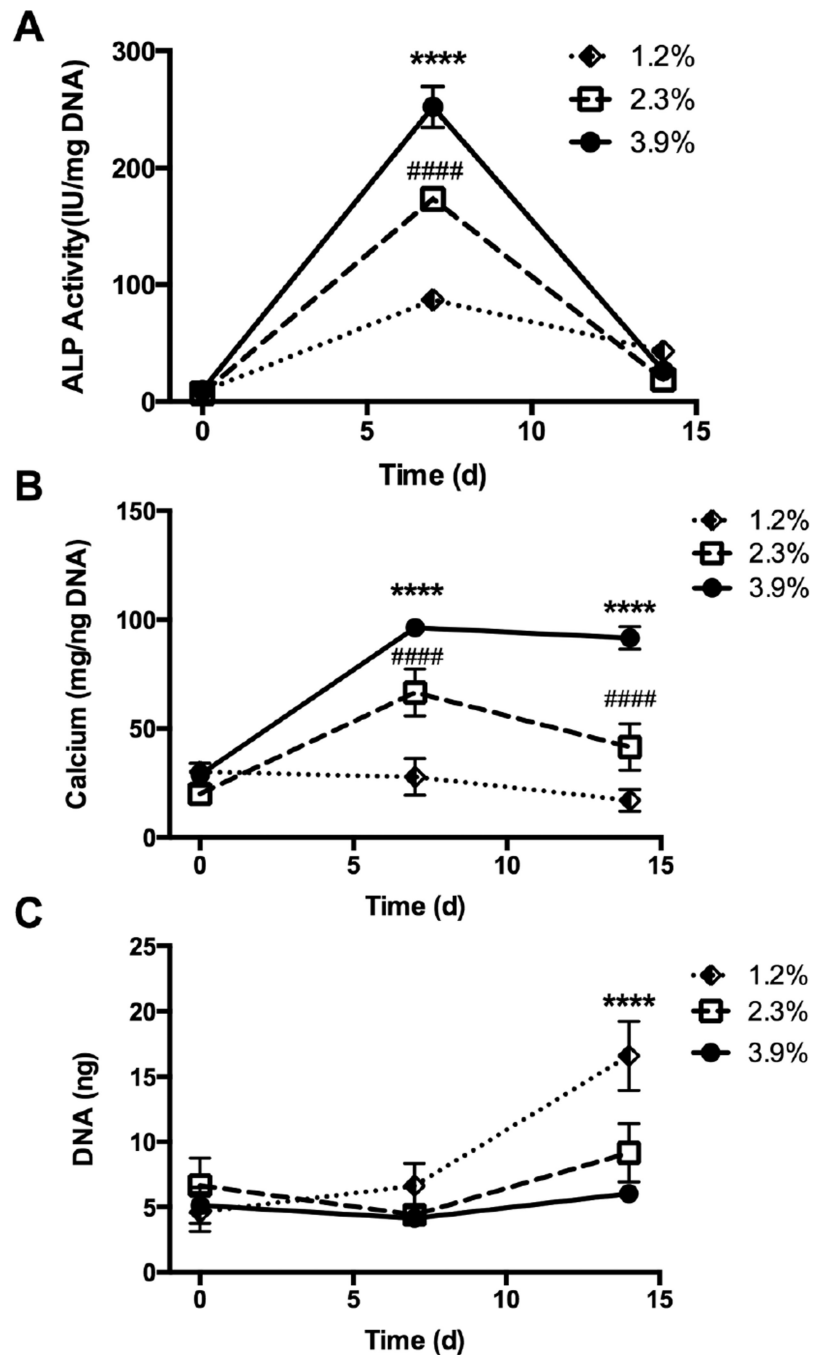


Figure 3. Fibrin gels with highest salt content induce greatest osteogenic response in entrapped MSCs *in vitro*. (A) ALP activity (n=4; **** p <0.0001 vs. 1.2% and 2.3%, #### p <0.0001 vs. 1.2% and 3.9%); (B) cell secreted calcium (n=4; **** p <0.0001 vs. 1.2% and 2.3%); and (C) DNA content (n=3; **** p <0.0001 vs. 1.2%).

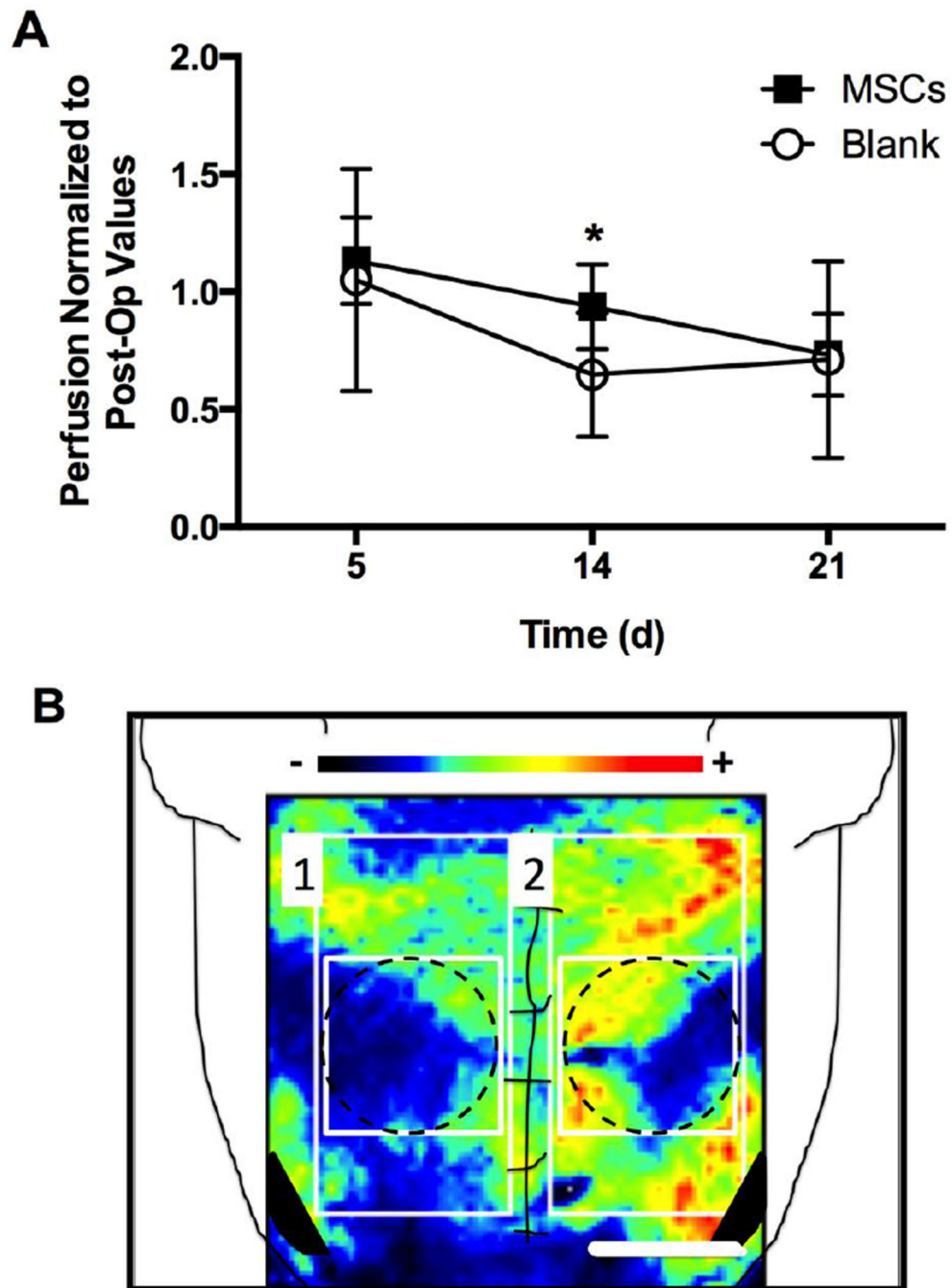


Figure 4. MSC-loaded gels increase vascular density in the calvarial defect. (A) Normalized perfusion relative to post-operative (Day 0) values ($*p < 0.05$ vs. blank gels); and (B) representative image of perfusion 14 days post-implantation. Side 1 = acellular blank fibrin gel; Side 2 = MSC-loaded fibrin gel. Scale bar represents 3 mm.

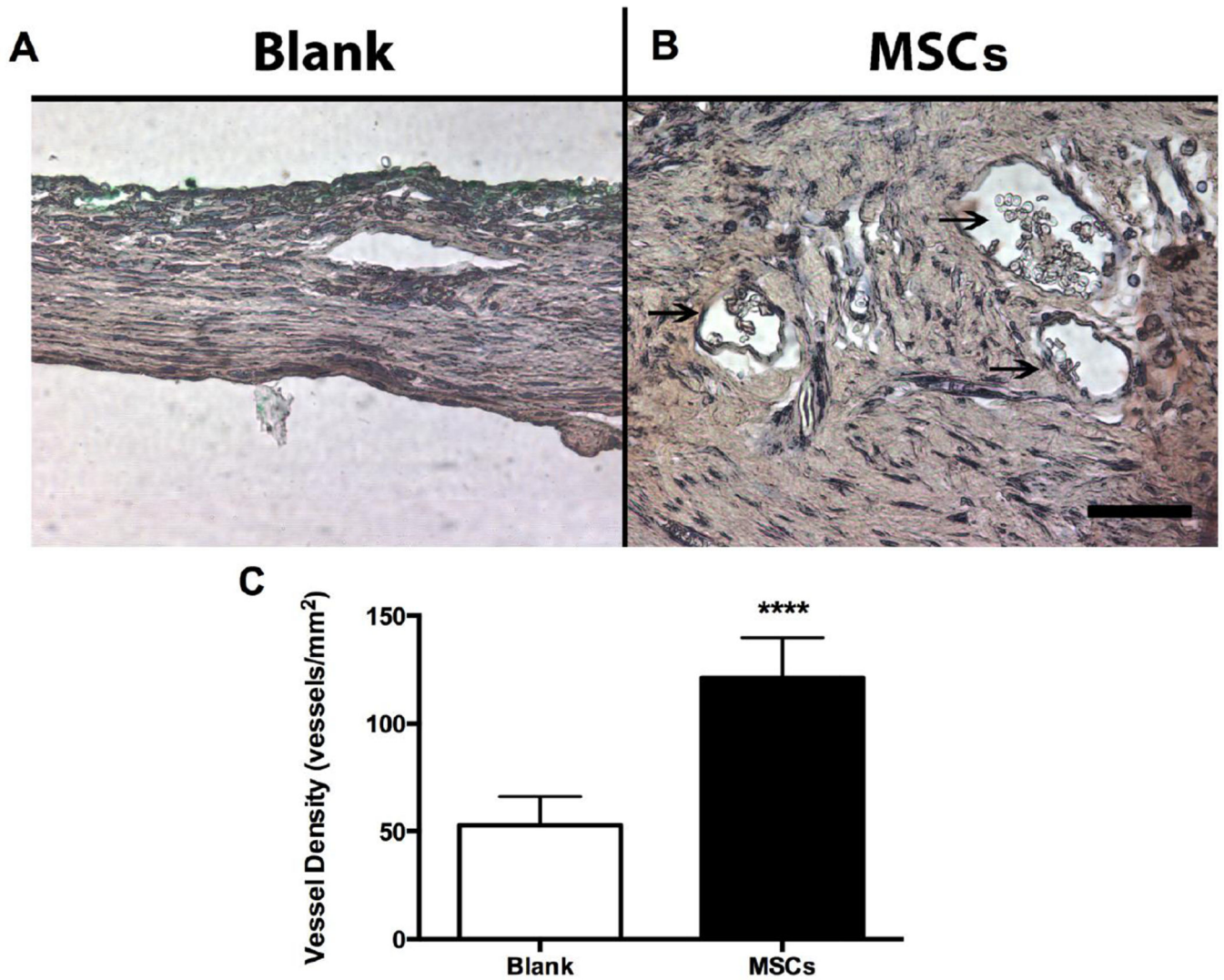


Figure 5. Repair tissue within calvaria 3 weeks post-implantation is more vascularized when treated with MSC-loaded fibrin gels. Representative CD31 stain of (A) blank gel and (B) MSC-containing gel near the center of the explant. Image at 40× magnification; scale bar represents 50 μm . (C) Vessel density within repair tissue (**** $p < 0.0001$ vs. blank gels, $n=6$).

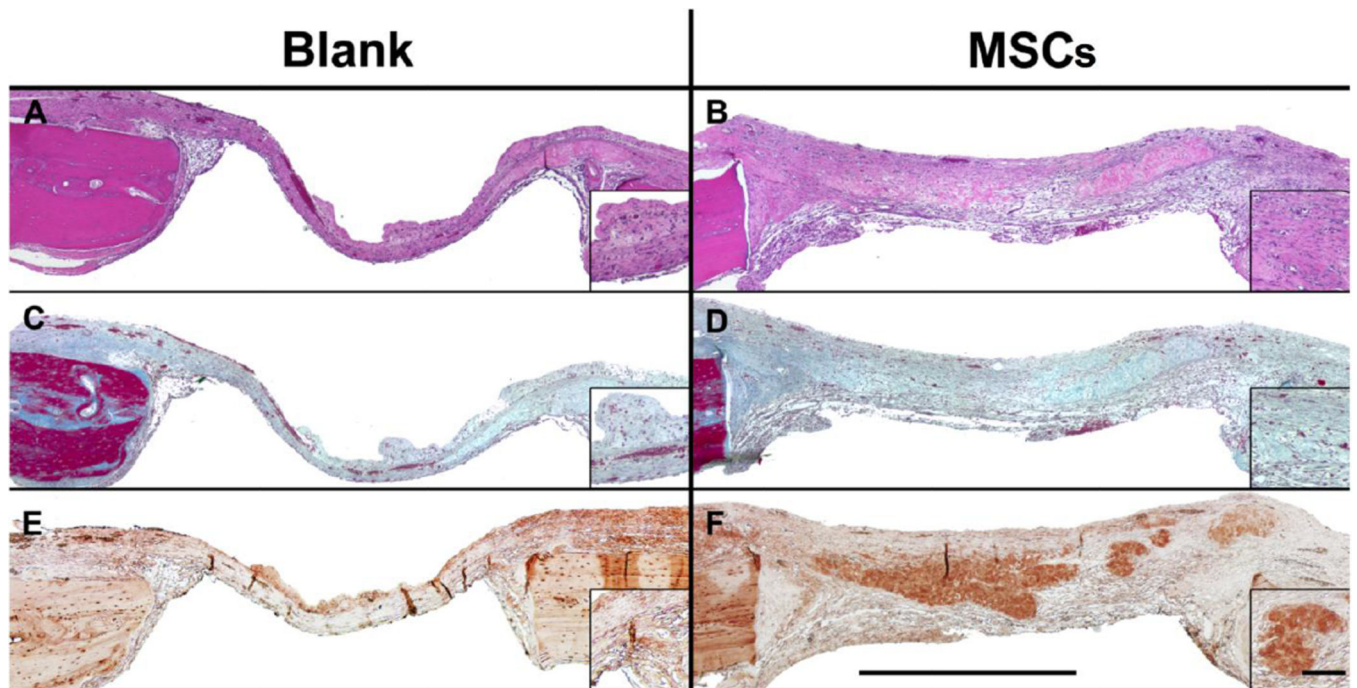


Figure 6.

Repair tissue within calvaria 3 weeks post-implantation is thicker with greater cellularity using MSC-loaded fibrin gels as demonstrated by representative stains of explants. (A) H&E stain of MSC-containing gel and (B) blank gel near the center of the explant; (C) Masson's Trichrome stain of MSC-containing gel and (D) blank gel near the center of explant; and (E) osteocalcin IHC of MSC-containing gel and (F) blank gel. Image at 10 \times magnification; scale bar represents 1 mm. Insets at 40 \times magnification; scale bar represents 100 μ m.

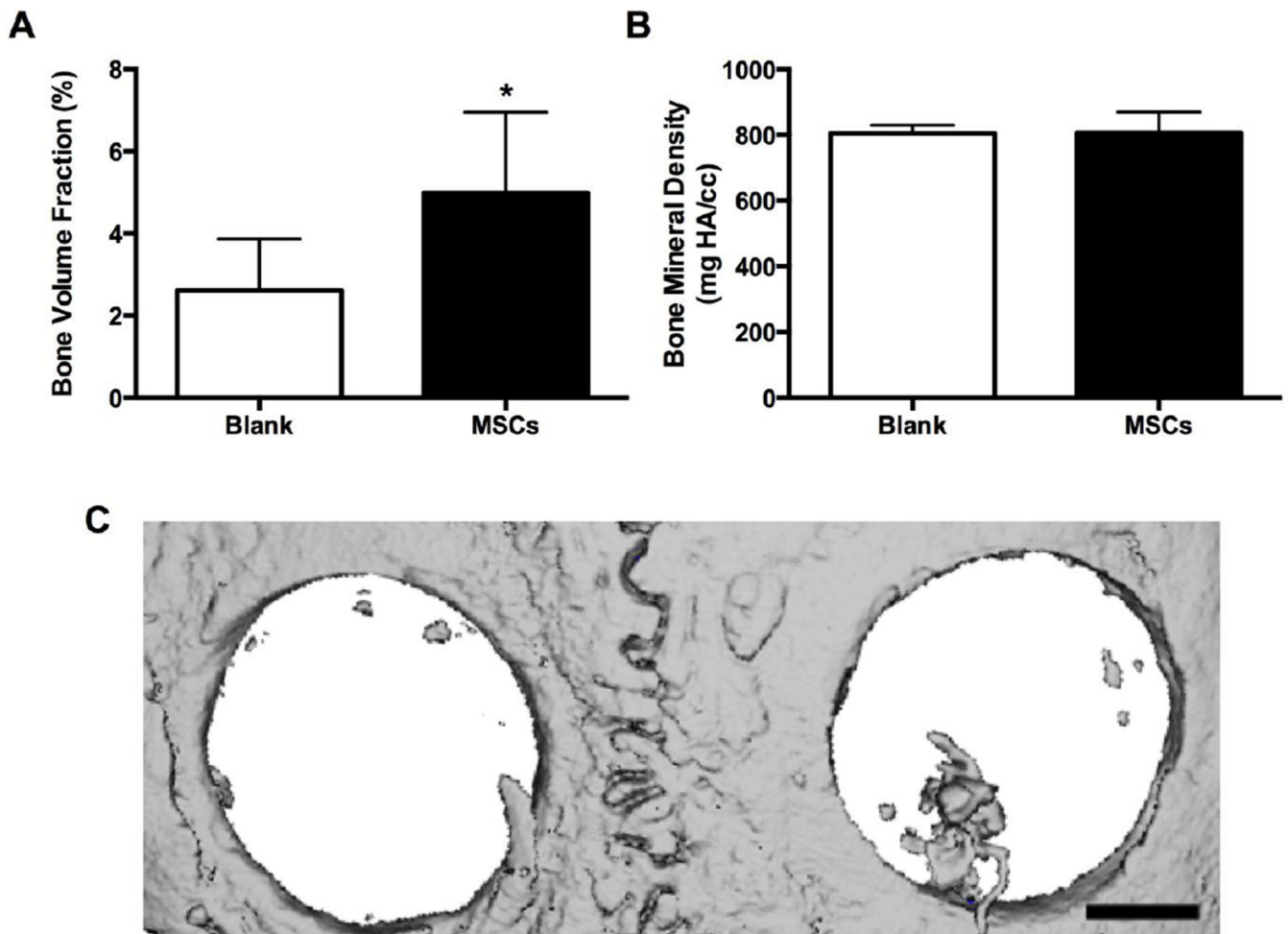


Figure 7. Characterization of bone quantity and quality within repair tissue after 12 weeks. (A) Bone volume fraction (BVF) is increased for defects treated with MSC-containing gels. (B) No difference in bone mineral density (BMD) was observed ($n=6$; $*p<0.05$ vs. blank gels). (C) Representative microCT image of bone formation in bilateral calvarial defect: acellular fibrin gel-treated defect is on the right, while MSC-treated defect is on the left. Scale bar represents 1 mm.